Polymer 59 (2015) 180–186

Contents lists available at ScienceDirect

Polymer

journal homepage: www.elsevier.com/locate/polymer

Phase behavior of model poly(butadiene 1,3)-*block*-(dimethylsiloxane) copolymers

Leopoldo R. Gómez [a], Daniel A. Vega [a, *], Mario Ninago [b], Andrés E. Ciolino [b], Marcelo A. Villar [b], Enrique M. Vallés [b]

[a] Instituto de Física del Sur – IFISUR, CONICET, Departamento de Física, Universidad Nacional del Sur (UNS), Av. Alem 1253, 8000 Bahía Blanca, Argentina
[b] Planta Piloto de Ingeniería Química, PLAPIQUI (UNS-CONICET), Camino La Carrindanga Km. 7, 8000 Bahía Blanca, Argentina

ARTICLE INFO

Article history:
Received 11 November 2014
Received in revised form
30 December 2014
Accepted 6 January 2015
Available online 12 January 2015

Keywords:
Anionic polymerization
High vacuum techniques
Model block copolymers

ABSTRACT

Model diblock copolymers of poly(butadiene-1,3) and poly(dimethylsiloxane) (PB-*b*-PDMS) of different compositions were synthesized by the sequential anionic polymerization (high vacuum techniques) of butadiene 1,3 and hexamethyl(ciclotrisiloxane), (D3), monomers. The block copolymers were characterized by nuclear magnetic resonance (^{1}H– and ^{13}C NMR), size-exclusion chromatography (SEC), Fourier Transform infrared spectroscopy (FTIR), and Small Angle X-ray Scattering (SAXS). SEC combined with ^{1}H NMR analysis indicate that the PB-*b*-PDMS copolymers exhibit molar masses between 5000 and 13000 g/mol, narrow polydispersity index (M_w/M_n), and chemical compositions ranging from low to intermediate siloxane content. According to SAXS experiments, at room temperature the model block copolymers present morphological arrangements that vary from disordered and body-centered-cubic packing of spheres, to hexagonally packed cylinders and lamellar structures.

1. Introduction

Block copolymers are macromolecules composed of two or more chemically distinct polymer blocks, covalently bounded [1–5]. In the last decades, different experiments performed in bulk or thin films have shown that even slightly dissimilar blocks can lead to nano-scale phase separated structures. Such phase separation processes spontaneously lead to self-assemble the copolymer into different ordered morphologies. In these systems, the molecular weight of the blocks controls the characteristic length scale of the structures (lattice parameter) while the volume fraction of each block sets the symmetry of the self-assembled morphology. In diblock A–B copolymers for example, depending upon its molecular weight and relative volume fractions, self-assembled structures with body centered cubic arrays of spheres, hexagonally packed cylinders, lamellar, and gyroid phases have been observed [1–5]. However, upon increasing the complexity of the molecular architecture a myriad of new morphologies can be obtained [6].

For many years self-organization has captured the interest of the scientific community because of the richness of emerging equilibrium and dynamical behavior [7]; also because it provides a powerful tool to produce useful and novel materials. From a technological perspective, self-assembled materials also offer a low cost and efficient route to nanofabrication [8–16]. Among various self-assembling materials, block copolymer are of particular technological interest because these materials self-assemble at length scales that are not accessible to traditional optical lithographic techniques [13].

In general, block copolymers with a high degree of molecular and compositional homogeneity (model polymers) are required to obtain highly regular phase separated structures. High vacuum anionic polymerization techniques offer a powerful method to synthesize model block copolymers with controlled macromolecular architectures [17–19]. In particular, the synthesis of block copolymers based on dimethylsiloxane has been achieved by using different synthetic strategies [20,21]. In a previous paper we have studied the order–order and order-disorder transitions in a model diblock copolymer of poly(butadiene-1,3) and poly(-dimethylsiloxane) (PB-*b*-PDMS) [22]. In this system, X-ray small angle scattering analysis (SAXS) combined with rheological experiments showed that the order–order and order-disorder transitions were thermoreversible. In this paper we extend our

* Corresponding author. Tel.: +54 2914595101.
E-mail addresses: dvega@uns.edu.ar (D.A. Vega), aciolino@plapiqui.edu.ar (A.E. Ciolino).

http://dx.doi.org/10.1016/j.polymer.2015.01.011
0032-3861/

previous studies regarding the phase behavior of several *model block* copolymers of the same family with different compositions.

We focus our interest in block copolymers based on dimethylsiloxane because PDMS as homopolymer exhibits a low glass transition temperature (T_g ~ −125 °C); unique flexibility; very low loss tangent; high dielectric strength; small temperature variations of the physical constants; high gas permeability; high compressibility; thermal stability over a wide range of temperatures; high lubricity; low chemical reactivity; and, essentially, a non toxic nature [23]. The incorporation of a PDMS segment into a common diene polymer allows the synthesis of thermoplastic elastomers [24], which could be easily obtained by the hydrogenation of the PB block [25]. However, as a first step, it is worth exploring the self-organization of the former copolymer (PB-*b*-PDMS) that might offer valuable information regarding nanostructures formed by the material.

In this study the PB-*b*-PDMS copolymers were synthesized using sequential addition of monomers, employing high–vacuum anionic polymerization techniques [17–19]. The molar masses of these copolymers were chosen in order to fall into the weak to intermediate regime of phase segregation and where the transitions from a spatially homogenous (disordered) state to a microphase-separated (ordered) state occurs close room temperature in order to minimize the PB degradation during annealing. The *block* copolymers so obtained were characterized by nuclear magnetic resonance (^{1}H– and ^{13}C NMR), size-exclusion chromatography (SEC), Fourier Transform infrared spectroscopy (FTIR), while the phase behavior and equilibrium structures were determined through SAXS.

2. Experimental

2.1. Materials

All materials were purified by standard anionic polymerization procedures [18]. The initiator *sec*–Butyl lithium (*sec*–Bu$^-$Li$^+$) was prepared *in vacuo* from *sec*–butyl chloride and lithium metal. Tetrahydrofuran (THF) was used as promoter for the hexamethyl(cyclotrisiloxane) monomer (D_3) polymerization. It was purified by fractional distillation, first over CaH_2 and then over sodium–potassium alloy. Cyclohexane and degassed methanol were used as the solvent and terminating agent, respectively. The purification of D_3 monomer (Aldrich, 98%) was performed as follows: in a flask, the appropriate amount of D_3 was melted, diluted by an equal volume of purified cyclohexane, and stirred over calcium hydride (CaH_2) overnight. The solvent, along with the monomer, was subsequently transferred to another flask containing poly(styryllithium) (PS$^-$Li$^+$). The monomer was allowed to stand in contact with PS$^-$Li$^+$ for about 2 h at room temperature, and was then distilled along with the solvent into a cylinder and divided into pre-calibrated ampoules.

The 1,3-Butadiene monomer (Bd) was first condensed in a graduated cylinder containing 5 mL of a commercial *n*-buthyl lithium solution (*n*-Bu$^-$Li$^+$) at −78 °C (dry ice/isopropanol bath). It was then stirred for 30 min at −10 °C (ice/salt bath) until the viscosity of the solution increased. Then, it was distilled again into a graduated cylinder at −78 °C, diluted with an appropriate volume of purified cyclohexane (ratio of [monomer]/[solvent] lower than 0.2) and divided into pre-calibrated ampoules.

2.2. Synthesis of PB-b-PDMS diblock copolymers

All manipulations were performed under high vacuum in glass reactors equipped with break–seals for the addition of the reagents and constrictions for removal of products [17,18]. The synthesis of PB-*b*-PDMS was achieved by sequential anionic polymerization as already reported [20].

In short: Ampoules of Bd and D_3 monomers, *sec*–Bu$^-$Li$^+$ solution, THF and degassed methanol were attached to the main polymerization apparatus as shown in Fig. 1 below. The apparatus was connected to the vacuum line, checked for pinholes, flame-dried and pumped for 20–30 min in order to remove the volatile species. Then, 5 mL of concentrated *n*-Bu$^-$Li$^+$ solution in hexane were injected via septum (a) into the purge section flask. The constriction of (a) was flame sealed, and the whole apparatus was pumped for an additional 30 min in order to remove hexane and air inserted during the injection. Then, an appropriate amount of pure cyclohexane (40–50 mL) was distilled and degassed over 45 min. The apparatus was removed from the vacuum line by heat sealing constriction (b), and washed with the diluted *n*-Bu$^-$Li$^+$ solution inside by gentle manual agitation. After washing, the solvent was distilled into reactor (D), and the purge section was removed by heat sealing constriction (c) leaving the clean reactor with an appropriate amount of pure cyclohexane.

The break-seal of the butadiene monomer solution was first broken, and the content was poured into the reactor flask followed by addition of the *sec*-Bu$^-$Li$^+$ ampoule. Both ampoules were rinsed with the solution in order to remove any traces of initiator or monomer, and the polymerization was left to proceed until all the monomer was consumed (usually, 24 h). An ampoule of living PB was then collected for further characterization.

After sampling the PB homopolymer, the ampoule containing D_3 was broken and rinsed with the living polymer solution, and the reaction was left to proceed for 20 h at room temperature. Subsequently, the THF ampoule was broken in order to promote D_3 polymerization. This polymerization was carried out in two steps: first, at room temperature for 3.5 h, and then at 30 °C for additional 24 h [26]. The living PB-*b*-PDMS copolymer chains were then terminated by adding an excess of well-degassed methanol. Although chlorosilanes are commonly used as terminating agents for cyclic organic siloxane monomers [27–29], it has been found that they suffer hydrolysis reactions with atmospheric humidity [30]. In addition, since the chlorosilane agent is used in excess, it is highly probable that the hydrochloric acid produced during the reaction promotes redistribution reactions of the poly(siloxane) chains [31].

PB-*b*-PDMS copolymers were precipitated in methanol (stabilized with 2,6-di-tert-butyl-p-cresol), dried under vacuum and characterized.

3. Characterization

3.1. Size exclusion chromatography (SEC)

The SEC experiments were performed on a Waters model 410 differential refractometer (equipped with 6 columns with a porosity range of 10^2–10^6 Å) in toluene at 25 °C with a flow rate of 1 mL/min and an injection volume of 200 μL, calibrated with polystyrene standards.

3.2. Nuclear magnetic resonance (^{1}H–NMR)

The ^{1}H NMR spectra of PB-*b*-PDMS copolymers were recorded on a Brucker 400 MHz instrument using deuterated chloroform as solvent. The chemical composition of the PB-*b*-PDMS copolymers was obtained by the ratio of the integrated areas of the vinyl to methylic ^{1}H signals.

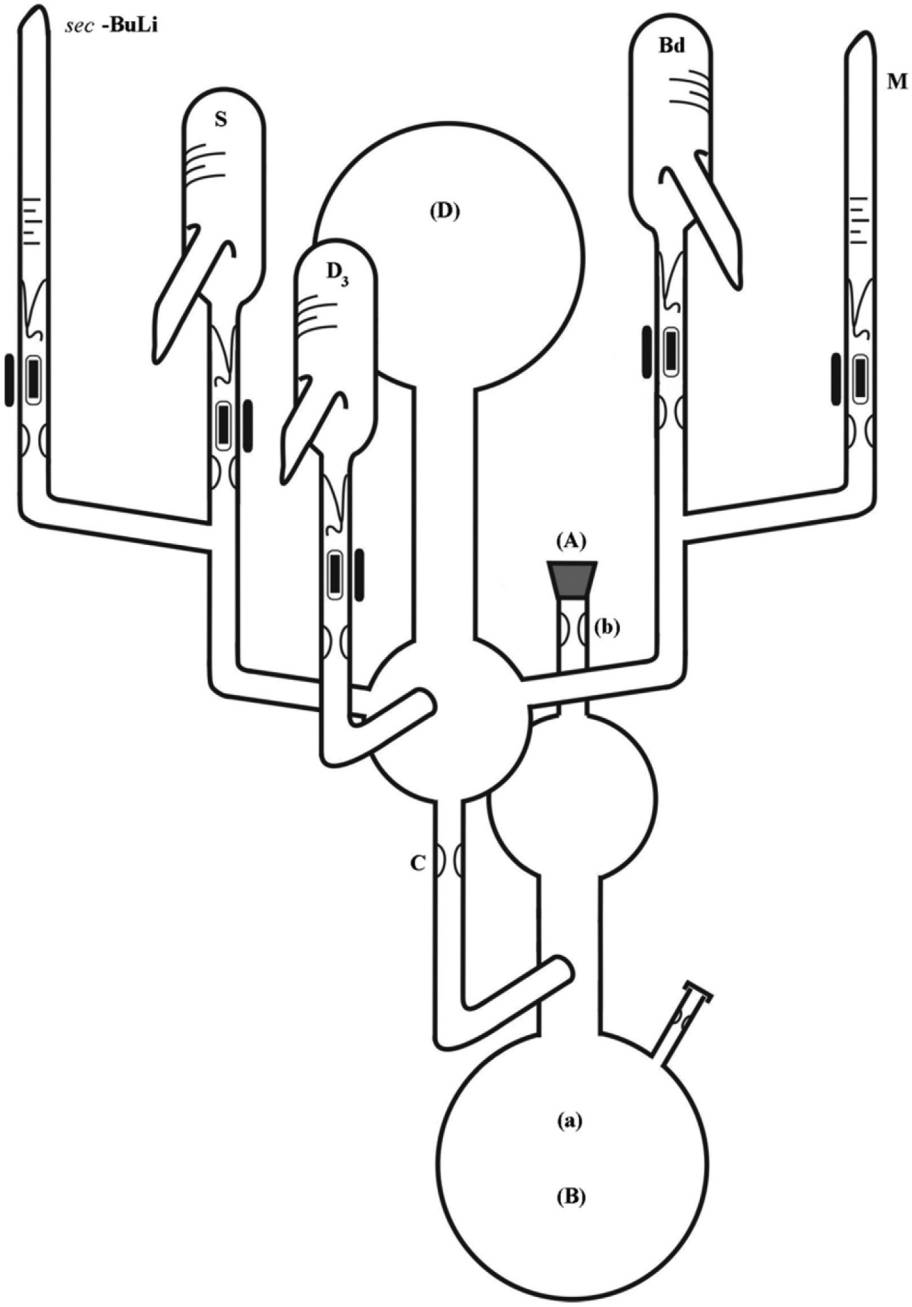

Fig. 1. Copolymerization apparatus. References: (A) Vacuum line connection. (a): Purge injection. (B): Purge flask. (b) and (c): Constrictions for heat-sealing. (D): Main polymerization reactor. (S): THF ampoule. (Bd): Butadiene 1,3 ampoule. (D_3): Hexamethyl(cyclotrisiloxane) ampoule and (M): Methanol ampoule.

3.3. Fourier Transform infrared spectroscopy (FTIR)

The FTIR spectra of the resulting polymers were obtained on a *Nicolet FTIR 520* spectrometer using cast films from diluted copolymers' solutions (1 wt% in hexane).

3.4. SAXS

The measurements were carried out at the "Brazilian Synchrotron Light Laboratory – LNLS" (Campinas, Brazil), on the beamline D11A-SAXS, the wavelength of the X-rays being 0.1488 nm. A collimated X-ray beam was passed horizontally through a chamber containing the sample, under vacuum. Data were collected on a CCD area detector placed at 1500 mm from the sample covering the momentum transfer q ranging from 0.09 to 2.25 nm^{-1}. Measurements were performed at different temperatures with an exposure time of 5 min.

4. Results and discussion

As we described in the previous section, the synthesis of PB-*b*-PDMS copolymers involves a sequential monomer addition. First, the polymerization of butadiene 1,3 with *sec*-$Bu^{-}Li^{+}$ as initiator that was carried out for 24 h to ensure the complete conversion of butadiene 1,3 to PB. Then, the polymerization of D_3 monomer until a complete polymerization. Following this methodology, we obtained a set of eight PB-*b*-PDMS diblock copolymers with different compositions and molar masses (see Table 1).

Table 1
SEC and ^{1}H NMR results for the PB-*b*-PDMS diblock copolymers and the corresponding PB and PDMS blocks.

Polymer	M_n teor.[a] (g/mol)	M_n[b] (g/mol)	M_n/M_w[b]	M_n PDMS[b] (g/mol)	x_{PDMS}[c]	w_{PDMS}[c]
PB1	12,000	10,700	1.07	–	–	–
DB1	13,000	11,700	1.04	1000	0.062	0.083
PB2	12,000	11,300	1.03	–	–	–
DB2	13,000	12,700	1.04	1400	0.083	0.110
PB3	7500	7400	1.03	–	–	–
DB3	10,000	9400	1.05	2000	0.171	0.220
PB4	9750	9500	1.03	–	–	–
DB4	12,400	11,700	1.05	2200	0.147	0.191
PB5	4500	4700	1.04	–	–	–
DB5	8000	7900	1.02	3200	0.330	0.403
PB6	5250	5400	1.06	–	–	–
DB6	8500	9200	1.02	3800	0.337	0.410
PB7	3000	2700	1.05	–	–	–
DB7	6000	5500	1.06	2800	0.422	0.500
PB8	3000	3700	1.04	–	–	–
DB8	7000	8300	1.03	4600	0.471	0.550

[a] Expected molecular weight according to stoichiometry.
[b] Molar mass and molar masses distribution relative to poly(styrene) standards (SEC at 298 K using toluene as solvent).
[c] Calculated from ^{1}H NMR spectra (298 K, $CDCl_3$ as solvent).

Fig. 2 shows representative SEC chromatograms of PB precursor and the corresponding PB-*b*-PDMS copolymer for run # 4, (DB4). Both the PB precursor and the corresponding PB-*b*-PDMS copolymer show a narrow molecular weight distribution (*e.g.* polymers with high structural homogeneity). The displacement of the PB-*b*-PDMS chromatograph towards lower elution volumes is a clear evidence of a higher molar mass obtained in the copolymer. From the analysis of the SEC chromatographs of both, PB and PB-*b*-PDMS copolymers, the molar masses and the molar masses distribution were calculated.

The chemical characterization of the samples was completed by analyzing their ^{1}H NMR spectra. Since the resonance peaks of ^{1}H from the methyl groups directly bonded to the silicon atoms ($-OSi(CH_3)_2$) of the PDMS block appear far from the corresponding resonance peaks assigned to the contribution of ^{1}H from 1,2– and 1,4– addition units of the PB block [25], the molar and weight fraction of PDMS in the corresponding PB-*b*-PDMS copolymers (x_{PDMS} and w_{PDMS}, respectively) can be easily calculated by the ratio of the corresponding integrated peak areas. Table 1 summarizes all the experimental results obtained from SEC and ^{1}H NMR analysis for PB-*b*-PDMS copolymers and PB precursors.

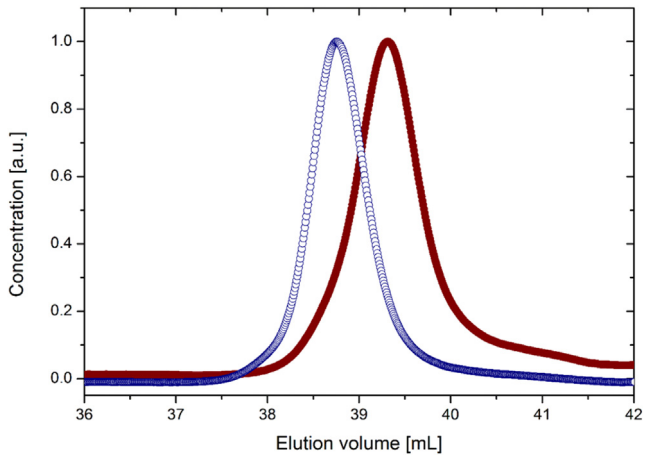

Fig. 2. Size exclusion chromatograms (SEC). Symbols: (fx2) PB 4 and (fx3) DB 4.

As one can deduce from the data reported above, the polydispersity indexes (M_w/M_n) of the samples is relatively small, and the chemical composition of the copolymers varies from low (DB1) to medium PDMS content (DB6). The representative SEC chromatograms shown in Fig. 2 reveal that the PB block and the corresponding PB-*b*-PDMS copolymer show a narrow distribution of molar masses, which is indicative of polymers with high structural homogeneity. As an additional information, the analysis of the FTIR spectra of the PB-*b*-PDMS show characteristic absorption bands at 1261 cm^{-1} (symmetric $-CH_3$ deformation in $Si-CH_3$ bonds), 1094 cm^{-1} and 1022 cm^{-1} (asymmetric Si–O–Si stretching vibrations); and at 802 cm^{-1} (Si–C stretching vibration), which reveal the presence of the PDMS block in the corresponding copolymers [32].

It is important to emphasize that the molecular weights reported in Table 1 are derived from elution times in a system calibrated with linear polystyrene standards. However, at the same molecular weight and SEC conditions, the poly(butadiene) and poly(styrene) have different hydrodynamic volumes (see, for example, Ref. [33]). Then, although Table 1 indicates that there is a good agreement between the theoretical and measured M_n values, differences between the apparent and true molecular weight can be expected.

4.1. Small angle X-ray scattering experiments

In this section we report synchrotron SAXS measurements of the different diblock copolymers described in Table 1. In order to emphasize the dominant features of the different block copolymer architectures, SAXS data are presented in three different figures, according to their relative block copolymer composition.

Fig. 3 shows the SAXS profiles observed at room temperature for samples DB1, DB2 and DB3. The block copolymer with the highest compositional asymmetry, DB1, shows no indication of order. Despite the thermodynamic incompatibility between the blocks, the very small volume fraction of the PDMS block locates this system in the one-phase side of the phase diagram. However, as shown in Fig. 4, upon decreasing the temperature from 298 K to 283 K, the SAXS data of the DB1 copolymer reveals the presence of a broad maximum and the occurrence of compositional fluctuations

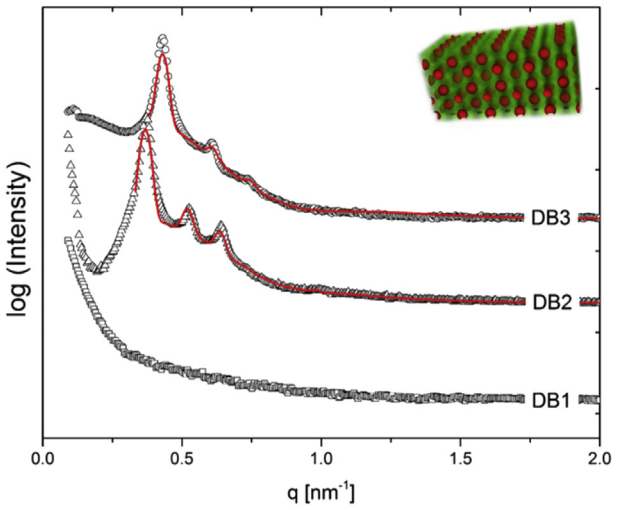

Fig. 3. SAXS patterns at T = 298 K for the PB-*b*-PDMS copolymers DB1, DB2 and DB3. Solid lines correspond to the fits of the experimental data to the theoretical scattering functions proposed by Forster et al. [24] for the microphase separated diblocks DB2 and DB3. Inset: schematic representation of the BCC packing of PDMS spheres embedded in a PB matrix. Profiles are shifted along the intensity axis for clarity.

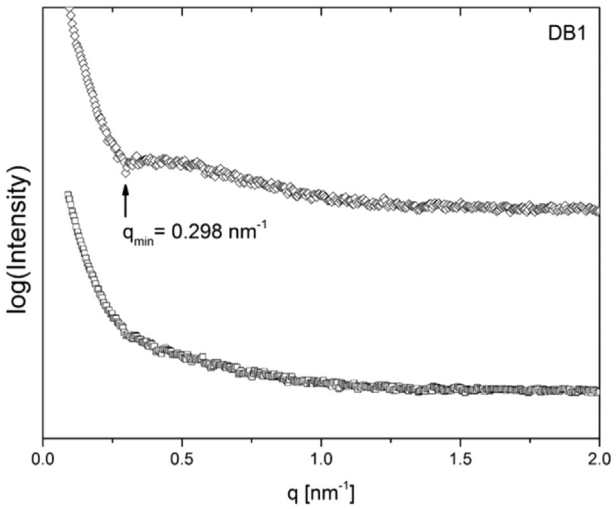

Fig. 4. SAXS patterns for the PB-*b*-PDMS copolymers DB1at two different temperatures: T = 298 K (bottom) and T = 283 K (top). Observe the presence of a weak maximum in the scattering intensity for the system tested at T = 283 K. Profiles are shifted along the intensity axis for clarity.

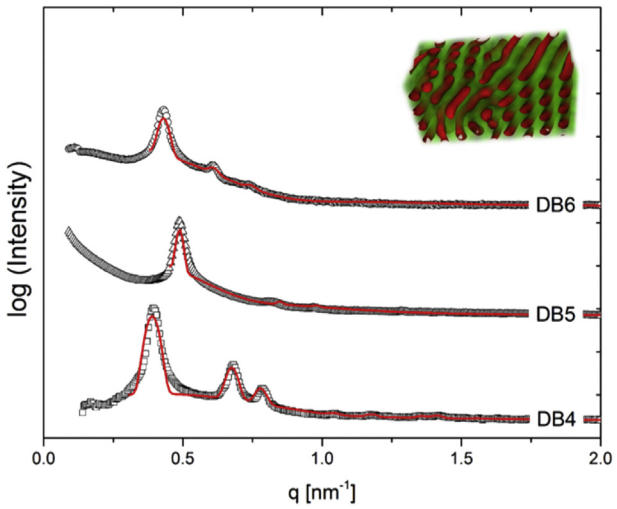

Fig. 5. SAXS patterns at T = 298 K for the PB-*b*-PDMS copolymers DB4, DB5 and DB6. Solid lines correspond to the fits of the experimental data to the theoretical scattering functions proposed by Förster et al. Inset: schematic representation of the hexagonal packing of PDMS cylinders embedded in a PB matrix. Profiles are shifted along the intensity axis for clarity.

that emerge as consequence of the thermodynamic incompatibility between the building blocks of the PB-*b*-PDMS copolymer [34,35].

By increasing the compositional asymmetry, SAXS data confirms that at room temperature samples DB2 and DB3 are in the BCC phase. In these samples up to three high order reflections are observed in positions q_m, $\sqrt{2}q_m$, $\sqrt{3}q_m$, $\sqrt{4}q_m$, with q_m, the main peak position ($q_m = 0.26$ nm^{-1}and $q_m = 0.305$ nm^{-1} for DB2 and DB3, respectively). Hence, from the compositional data shown in Table 1 and the SAXS patterns shown in Fig. 3 we can conclude that the morphology of these two copolymers corresponds to a BCC packing of PDMS spheres in the PB matrix.

Fig. 5 shows the SAXS spectrum for samples DB4, DB5 and DB6. Observe in this figure that at room temperature these polymers phase separate into cylinders with hexagonal packing, as revealed by the reflections with peak positions q_m, $\sqrt{3}q_m$, $\sqrt{4}q_m$ and $\sqrt{7}q_m$ [35]. In this case, the man peak positions appears at: $q_m = 0.39$ nm^{-1} (DB4),$q_m = 0.485$ nm^{-1} (DB5) and $q_m = 0.416$ nm^{-1} (DB6).

In Fig. 6 we compare the SAXS profiles for the block copolymer DB5 at two different temperatures, T = 298 K and T = 343 K. These data show that at T = 343 K this block copolymer develops a BCC structure, with PDMS spheres embedded in a PB matrix. In this case, the main SAXS reflections appears at positions q_m, $\sqrt{2}q_m$, $\sqrt{3}q_m$, $\sqrt{4}q_m$, with $q_m = 0.42$ nm^{-1}.

The order–order transition between hexagonal and BCC structures in diblock copolymers have been extensively studied in the past [34,36–38]. Theoretically, it has been proposed that upon increasing the temperature beyond the spinodal, the packing of spheres in a HEX-BCC transition proceeds through spatially correlated modulations along the cylinders of the minority phase [36]. According to this model, the ratio $q_m^{BCC}/q_m^{HEX} = 1.08$. From the positions of the primary Bragg peak for both structures, here we obtained $q_m^{BCC}/q_m^{HEX} = 0.42/0.39 = 1.07$, in good agreement with the theory.

Fig. 6 also compares the SAXS spectrum for the block copolymer DB5 at two different temperatures, T = 298 K and T = 323 K. Note that the main peak position in both spectra is located at similar values of the wave vector magnitude ($q_m = 0.42$ nm^{-1}). The SAXS spectrum at T = 323 K show a broad maximum with lack of higher order reflections. This spectrum is consistent with a system being in one phase, with the broad maximum in the SAXS profile arising from concentration fluctuations.

Fig. 7 shows the SAXS spectrum corresponding to the highly symmetric block copolymers DB7 and DB8. In this case, it can be observed that the main peak reflections appears evenly spaced at positions q_m,$2q_m$, $3q_m$, $4q_m$ consistent with a lamellar order. In this case, $q_m = 0.45$ nm^{-1} for DB7 and $q_m = 0.28$ nm^{-1} for the diblock copolymer DB8. Note that in both spectra the peaks corresponding to the even-order are significantly suppressed. This scattering patterns strongly indicates symmetric lamellar morphologies [35].

In order to obtain a more detailed information of the different morphologies, the SAXS results for the self-assembled structures presented in Figs. 3, 5 and 7 where analyzed by fitting the experimental curves to analytical expressions for the scattering intensity [35].

The scattering functions used to describe the experimental data have been developed by Förster et al. considering the contribution from the structure and form factors [35,39]. According to the scattering theory, the intensity of the SAXS data can be described as [35]:

$$I(q) = (b_1 - b_2)^2 \rho_N P(q) S(q) \quad (1)$$

where b_i is the scattering length of phase i, ρ_N is the number particle density, $P(q)$ is the form factor and $S(q)$ corresponds to the structure factor. The expressions for the form factor take into account particle size distributions, characterized by the domain size D, its polydispersity σ_d, and characteristic size of the scattering object (R). The structure factor $S(q)$ is determined, for a given scatters packing, by a characteristic unit cell dimension a that can be estimated from the Bragg peaks position.

The fit with analytical expressions for the scattering functions are presented in Figs. 3, 5 and 7 as continuous lines. It can be observed that the theoretical curves provide a reasonably good description to the experimental data and that also capture the symmetry and dominant features of the morphology for different block copolymers.

Table 2 shows the parameters extracted from fits of the SAXS data for the samples DB2 through DB8. The fitting parameters include: average lattice constant (a), the domain size D and its standard deviation (σ_d) and the characteristic size of the scattering object (R) (PDMS sphere radius for DB2 and DB3, cylinder radius for

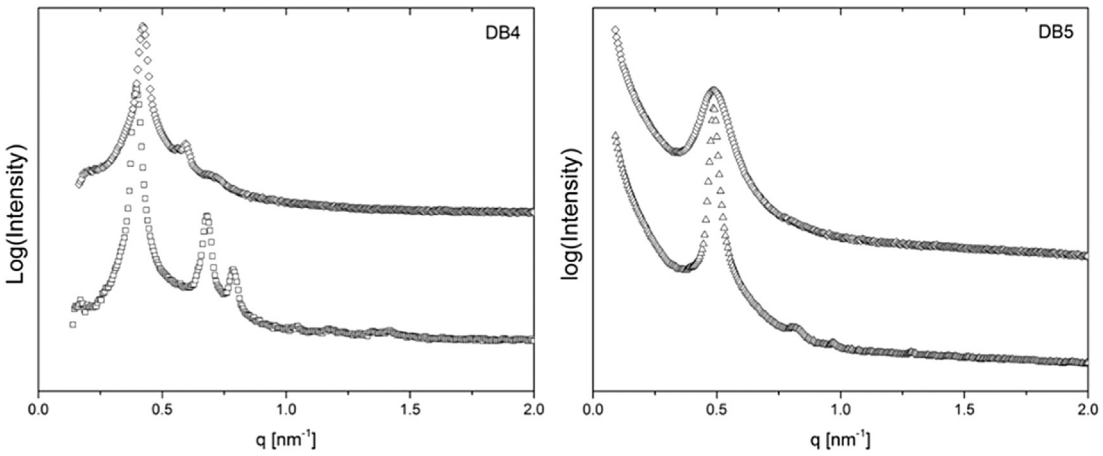

Fig. 6. SAXS patterns for the PB-*b*-PDMS copolymers DB4 (left) and DB5 (right) at two different temperatures. Upon increasing the temperature from T = 298 K (bottom pattern) to T = 343 K (top pattern), the diblock copolymer DB4 suffers a HEX-to-BB order–order transition. The diblock DB5 suffers an order-disorder transition upon increasing the temperature from T = 298 K (bottom pattern) up to T = 323 K (top pattern). Profiles are shifted along the intensity axis for clarity.

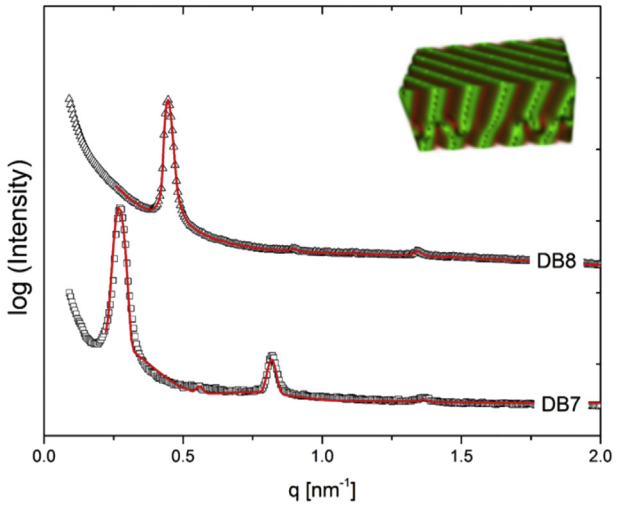

Fig. 7. SAXS patterns at T = 298 K for the PB-*b*-PDMS copolymers DB7 and DB8. Solid lines correspond to the fits of the experimental data to the theoretical scattering functions. Inset: schematic representation of the symmetric lamellar structure observer in these polymers Profiles are shifted along the intensity axis for clarity.

DB4, DB5 and DB6, and half of the average lamellar thickness of one component for the case of sample DB7 and DB8). Note in Table 2 that for the copolymers DB7 and DB8 $a \sim 4R$, that is in agreement with the features of the SAXS data shown in Fig. 7, showing that in these systems the volume fractions of each block are similar.

Table 2
Characteristics of the PB-PDMS diblocks obtained through the fits of the experimental data to the theoretical scattering functions (T = 298 K).

Polymer	ϕ_{PB}[a]	Morphology	a [nm]	D [nm]	σ_d [nm]	R [nm]
DB 1	0.92	Disordered	–	–	–	–
DB 2	0.887	BCC	24.0	175	2.9	5.7
DB 3	0.79	BCC	20.8	155	3.4	5.2
DB 4	0.82	Hex	18.5	139	1.1	4.2
DB 5	0.62	Hex	14.9	170	2.5	5.6
DB 6	0.613	Hex	17.5	188	2.1	5.4
DB 7	0.5	Lamellar	23.0	185	2.9	5.9
DB 8	0.474	Lamellar	13.7	210	2.3	3.8

[a] Volume fractions determined according to the densities detailed in Ref. [40]: $\rho_{PDMS} = 0.97$ gcm^{-3}, $\rho_{PBd} = 0.895$ gcm^{-3}.

5. Conclusions

Model PB-*b*-PDMS copolymers were synthesized by sequential anionic polymerization of butadiene 1,3 and D_3, using high-vacuum techniques. Sequential addition of monomers and a two-step methodology were applied, by which PB-*b*-PDMS copolymers with structural homogeneity and narrow molecular weight distributions were obtained. SAXS experiments combined with scattering theory allow to determine the equilibrium structures of the different block copolymer systems as well as the characteristic dimensions of the scatter centers. Although within the relatively narrow regime of temperatures explored here we have identified order–order and order disorder transitions, a more detailed analysis in terms of different annealing conditions is required in order to explore the kinetics leading to the different structures and the equilibrium properties of the different diblock copolymers.

Acknowledgments

We express our gratitude to the Brazilian Synchrotron Light Laboratory LNLS (D11A- SAXS1-8599), the Consejo Nacional de Investigaciones Científicas y Técnicas de la República Argentina (CONICET), the Agencia Nacional de Promoción Científica y Tecnológica (ANPCyT), and the Universidad Nacional del Sur (UNS, Argentina) for their financial support.

References

[1] Matsen MW, Schick M. Phys Rev Lett 1994;72:2660–3.
[2] Matsen MW, Bates FS. Macromolecules 1996;29:1091–8.
[3] Hamley IW. The physics of block copolymers. Oxford: Oxford University Press; 1998.
[4] Bates FS, Fredrickson GH. Phys Today 1999;52:32–8.
[5] Matsen MW. J Phys Condens. Matter 2002;14:R21–47.
[6] Bates FS, Hillmyer MA, Lodge TP, Bates CM, Delaney KT, Fredrickson GH. Science 2012;336:434–40.
[7] Seul M, Andelman D. Science 1995;267:476–83.
[8] Hamley IW. Nanotechnology 2003;14:R39–54.
[9] Ruzzette AV, Leibler L. Nat Mater 2005;4:19–31.
[10] Darling SB. Prog Polym Sci 2007;32:1152–204.
[11] Sik Y, Ross CA. Nano Lett 2007;7:2046–50.
[12] Albert JN, Epps TH. Mater Today 2010;6:24–33.
[13] Marencic AP, Register RA. Annu Rev Chem Biomol Eng 2010;1:277–97.
[14] Park S, Tsarkova L, Hiltl S, Roitsch S, Mayer J, Böker A. Macromolecules 2012;45:2494–501.
[15] Vega DA, Gómez LR, Pezzutti AD, Pardo F, Chaikin PM, Register RA. Soft Matter 2013;9:9385–91.

[16] García NA, Davis RL, Kim SY, Chaikin PM, Register RA, Vega DA. RSC Adv 2014;4:38412–7.
[17] Hadjichristidis N, Iatrou H, Pispas S, Pitsikalis MJ. Polym Sci Part A Polym Chem 2000;38:3211–34.
[18] Uhrig D, Mays JW. J Polym Sci Part A Polym Chem 2005;43:6179–222.
[19] a) Morton M, Fetters L. Rub Chem Tech 1975;48:359–409;
b) Bellas V, Iatrou H, Hadjichristidis N. Macromolecules 2000;33:6993–7;
c) Hadjichristidis N, Iatrou H, Pitsikalis M, Avgeropoulos A. Prog Polym Sci 2005;30:725–82.
[20] Ciolino A, Pieroni O, Vuano B, Villar MA, Vallés EM. J Polym Sci Part A Polym Chem 2004;42:2920–30.
[21] Baran DS, Akgün M, Akgün NA, Turk DS. J Chem 2004;28:645–57.
[22] Ciolino AE, Gómez LR, Vega DA, Villar MA, Vallés EM. Polymer 2008;49:5191–4.
[23] Lötters J, Olthuis W, Veltink P, Bergveld PJ. Micromech Microeng 1997;7:145–7.
[24] Almdal K, Mortensen K, Ryan A, Bates F. Macromolecules 1996;29:5940–7.
[25] Ciolino A, Sakellariou G, Pantazis D, Villar M, Vallés E, Hadjichristidis N. J Polym Sci Part A Polym Chem 2006;44:1579–90.
[26] Ninago M, Satti A, Ressia J, Ciolino A, Villar M, Vallés E. J Polym Sci Part A Polym Chem 2009;47:4774–83.
[27] Zilliox JG, Roovers JEL, Bywater S. Macromolecules 1975;8:573–8.
[28] Gerharz B, Wagner Th, Ballaufft M, Fischer EW. Polymer 1992;33:3531–5.
[29] Hardy CM, Bates FS, Kim M-H, Wignall GD. Macromolecules 2002;35:3189–97.
[30] Cella JA, Carpenter JC. J Organomet Chem 1994;480:23–6.
[31] Bontems SL, Stein J, Zumbrum MA. J Polym Sci A Polym Chem 1993;31:2697–710.
[32] Anderson D. In: Smith Lee, editor. Analysis of silicones. New York: John Wiley & Sons; 1974.
[33] Sebastian JM, Register RA. J Appl Polym Sci 2001;82:2056–69.
[34] Li M, Liu Y, Nie H, Bansil R, Steinhart M. Macromolecules 2007;40:9491–502.
[35] Förster S, Timmann A, Konrad M, Schellbach C, Meyer A, Funari SS, et al. J Phys Chem B 2005;109:1347–60.
[36] Matsen MW. J. Chem Phys 2001;114:8165–73.
[37] Laradji M, Shi A-C, Noolandi J, Desai RC. Macromolecules 1997;30:3242–55.
[38] Kimishima K, Saijo K, Koga T, Hashimoto T. Macromolecules 2013;46:9032–44.
[39] Förster S, Apostol L, Bras W. J Appl Crystallogr 2010;43:639–46.
[40] Fetters LJ, Lohse DJ, Richter D, Witten TA, Zirkel A. Macromolecules 1994;27:4639–47.